Shelby Rustom
Center for Advanced Vehicular Systems,
Mississippi State University,
Starkville, MS 39759
e-mail: shelbyrustom@gmail.com

YubRaj Paudel[1]
Center for Advanced Vehicular Systems,
Mississippi State University,
Starkville, MS 39759
e-mails: yp105@msstate.edu;
yubraj@cavs.msstate.edu

Shiraz Mujahid
Center for Advanced Vehicular Systems,
Mississippi State University,
Starkville, MS 39759
e-mail: shiraz@cavs.msstate.edu

Matthew Cagle
Center for Advanced Vehicular Systems,
Mississippi State University,
Starkville, MS 39759;
Department of Mechanical Engineering,
Mississippi State University,
Mississippi State, MS 39762
e-mail: mc1092msu@gmail.com

Prathmesh Anantwar
Mechanical and Aerospace Department,
University of Alabama in Huntsville,
Huntsville, Al 35899
e-mail: prathmesh.anantwar@uah.edu

Kavan Hazeli
Mechanical and Aerospace Department,
University of Alabama in Huntsville,
Huntsville, Al 35899
e-mail: hazeli@arizona.edu

Robert Moser
US Army Corps of Engineers,
Vicksburg, MS 39180
e-mail: Robert.D.Moser@usace.army.mil

Bhasker Paliwal
Center for Advanced Vehicular Systems,
Mississippi State University,
Starkville, MS 39759
e-mail: paliwb@rpi.edu

Hongjoo Rhee
Center for Advanced Vehicular Systems,
Mississippi State University,
Starkville, MS 39759;
Department of Mechanical Engineering,
Mississippi State University,
Mississippi State, MS 39762
e-mail: hrhee@me.msstate.edu

Manufacturing Strategies to Mitigate Deformation Twinning in Magnesium

Magnesium (Mg) alloys exhibit poor room temperature ductility, which prohibits forming operations in cost-effective industrial settings and the use of these alloys in critical safety components. Profuse twinning in Mg alloys is widely associated with high strain path anisotropy and low material ductility. Twinning typically propagates across the grains through the autocatalysis phenomena in typical texture conditions. Twin–twin and twin–slip interactions often lead to high strain incompatibilities and eventually failure. One way to avoid such premature failure is to prevent the early nucleation of twins. This research tests a hypothesis that a strong yet ductile phase surrounding each individual grain in traditional polycrystals could inhibit twin accommodation effects and thus twin nucleation and autocatalysis mechanisms at grain boundaries. As a proof-of-concept for testing this hypothesis, sharply textured magnesium sheets plated with different materials were subjected to four-point bending to assess the potential of a surface/grain boundary barrier in limiting twinning extent. The results showed that Mg AZ31 alloy plated with zinc alleviated twin nucleation while improving the strength of the alloy.
[DOI: 10.1115/1.4056553]

Keywords: material modeling, material performance and applications, materials, metallic materials, microstructure, microstructure property relationships

[1]Corresponding author.
Manuscript received May 13, 2022; final manuscript received December 15, 2022; published online January 5, 2023. Assoc. Editor: Przemyslaw Gromala.

Haitham El Kadiri
Center for Advanced Vehicular Systems,
Mississippi State University,
Starkville, MS 39759;
Department of Mechanical Engineering,
Mississippi State University,
Mississippi State, MS 39762;
Universite Internationale de Rabat,
Rabat-Shore Rocade Rabat-Salé,
Rabat 11103, Morocco
e-mail: elkadiri@me.msstate.edu

Christopher D. Barrett
Center for Advanced Vehicular Systems,
Mississippi State University,
Starkville, MS 39759;
Department of Mechanical Engineering,
Mississippi State University,
Mississippi State, MS 39762
e-mail: barrett@me.msstate.edu

1 Introduction

Magnesium (Mg) and its alloys have the potential to be promising engineering platform materials due to their high strength-to-weight and stiffness-to-weight ratios and their affordability compared to other lightweight materials such as carbon fiber. However, due to a low ductility at room temperature and predominantly brittle failure resulting from the hexagonal closed packed (HCP) crystalline structure, Mg alloys are difficult to incorporate into a commercial setting [1–3]. Thus, understanding the deformation mechanisms that drive microstructural evolution and influence ductility is critical to enable optimization of the Mg alloy composition and microstructure. Moreover, determining whether brittle failure in HCP lattice structures can be mitigated is crucial for producing a stronger, more ductile form of magnesium.

The low ductility of Mg alloys ultimately results from a lack of easy slip systems, which is innate to the HCP lattice. Like many HCP metals, Mg has an easy slip mode along the basal planes; however, the stress required to slip along the prismatic and pyramidal planes is orders of magnitude higher. The five independent slip systems required by Taylor criterion for arbitrary ductile shape change are not generally all operable at temperatures below 300 °C. At lower temperatures, while the basal slip is easy, extension and contraction of the $\langle c \rangle$ axis are difficult [4]. Due to this inability to initiate slip at room temperature, as well as the HCP lattices' low symmetry, deformation twinning is promoted rather than $\langle c+a \rangle$ slip [5,6].

Deformation twinning is frequently observed in Mg and is a mechanism that accommodates plastic strain along the $\langle c \rangle$ axis, as well as $\langle c+a \rangle$ dislocation gliding [7,8]. It has long been known that the $\{10\bar{1}2\}\langle 10\bar{1}1 \rangle$ tension twin, as well as the $\{10\bar{1}1\}\langle 10\bar{1}2 \rangle$ compression twin, plays a very important role in deformation mechanisms in Mg as well as other HCP materials [9,10]. Twinning accommodates plastic strain; the reorientation of grains due to twinning has been suggested to promote dislocation gliding, and thus plastic straining [11–13]. Twin advancement is controlled by two processes: nucleation and growth. The nucleation of twins usually originates at the grain boundary and continues to propagate across the grain. Twin growth occurs by way of fast extension of a sharp twin tip and is then followed by a coordinated slower migration of the boundaries [14]. Many factors can influence twinning; among these factors is grain boundary misorientation, which is hypothesized to have a substantial influence on the twinning stress magnitude as well as the twin propagation stress [15–17]. Twins which collide with low-angle grain boundaries generally induce the same twin system to activate in the opposite grain because of the similarity of the twinning shears and the resolved shear stresses in a phenomenon known as accommodation. This results in twin bands that can quickly span the entire material [4,18,19].

Twin nucleation sites in Mg alloy are preferred at low misorientation angle grain boundaries, which tend to be the highest energy boundaries [20]. Free surfaces are also prevalent nucleation sites for twinning. The material conditions required to nucleate twins have been studied extensively and are still unclear. However, it is well known that the nucleation site must have a pre-existing defect structure which helps stabilize the twin embryo when it is small. Additionally, the nucleation site must accommodate the twinning shear without inducing too much strain energy due to the eigenstrain of the twin. This condition may be satisfied by a free surface to accommodate the shear or easy basal slip or twinning across a grain boundary.

There have been many proposed methods attempting to inhibit twinning in HCP materials, including grain refinement to promote randomized textures and alloying designed to promote easier $\langle c+a \rangle$ slip [21,22] and texture randomization [23]. Additional work has focused on attempting to restrict twin boundary migration by promoting segregation to twin boundaries. Unfortunately, the success of these results has been too limited to result in widespread applicability. Therefore, in this work, we propose a new strategy for the suppression of the twinning mechanism.

The conditions required for twin nucleation are, in many ways, similar to those required to nucleate a crack. It is known that crack initiation strongly depends on the surface condition of a specimen's surface, and therefore crack initiation could be affected by a coating [24,25]. There are currently many applications for Mg coating treatments such as anodizing [26], conversion coating [27], as well as electroplating and electrolysis plating [28,29] and others. Mg alloys have previously been plated with chromium, copper, nickel, and niobium in attempts to inhibit corrosion as well as increase the strength and ductility [30–32]. Results from these previous studies showed that the electroplated Mg alloys produced improved surface hardness resulting in more plastic deformation resistance [30,31]; however the low-cycle fatigue life decreased for a Mg AZ61 alloy after alkaline Cu followed by acidic Cu, Ni/Cu, and Cr–C/Cu electroplating [31]. We hypothesize that this same process could be used to suppress twin nucleation on the surface. Twinning is accommodated at the free surface by kink formation [16,33]. Plating a sharply textured Mg alloy with other metals that can hinder such kink accommodation slows twin nucleation events, thus delaying the failure. A comparable study done in

a highly textured sample could suppress the formation of twin bands, thus possibly resulting in higher overall ductility. Our effort in this work is to test this hypothesis by observing the coating materials' effects on twin nucleation and propagation in a sharply textured Mg (MgAZ31).

2 Methodology

Rectangular magnesium samples of size 0.635 mm (t) × 152.4 mm (l) × 25.4 mm (w) were machine polished and then sent to C.I.L Electroplating Inc to be plated by zinc (Zn), copper (Cu), and nickel (Ni). The samples are oriented such that the transverse direction is along the length of the sample, the normal direction is along the height of the sample, and the rolling direction is aligned parallel to the width of the sample as shown in Fig. 1(*a*). Due to magnesium's propensity to chemically react, exceptions had to be made for certain types of plating to adhere to the matrix. Samples were dipped into electroplating baths, and some types of plating required a copper "prestrike" for adhesion. The HCP structured zinc plating adhered directly to Mg, but the face centered cubic (FCC) structured nickel and copper-plated samples required a prestrike. Other samples were sent to advanced surface technologies finishing, which underwent a chromium conversion process.

The experimental setup in Fig. 1(*a*) shows the magnesium sample inside a die, ready to perform four-point bending. Figure 1(*b*) shows a schematic of a four-point bending test with a symmetric loading of P/2 each applied at a distance of "L/4" from the outer fixtures. Samples were bent to 1%, 1.5%, and 2% strain (ε_{xx}) by way of four-point bending using the Instron 5882. The deflection required at loading points B and C (see Fig. 1) and maximum deflection at the middle of the sample to achieve these maximum strains were calculated using Eq. (1) [34].

$$\delta_{L/4} = \frac{L^2}{6H}\varepsilon_{xx} \quad \text{and} \quad \delta_{L/2} = \frac{11L^2}{48H}\varepsilon_{xx} \tag{1}$$

where L is the length between the outer pegs, H is the thickness of the sheet, and "ε_{xx}" is the flexural strain along x direction. The corresponding maximum compressive and tensile stresses on the upper and lower surfaces are given by

$$\sigma_{\max} = \mp\frac{3PL}{4WH^2} \tag{2}$$

where W is the width of the sample.

Separate plated samples were also analyzed using a digital imaging correlation (DIC) to determine the LaGrangian strain that each sample underwent locally. Samples were bent to 1% and 2% strains using the Universal Servo Hydraulic MTS Machine. The strain was measured using ASTM standard D6272, which agrees with Eq. (1).

3 Results and Discussion

Stress–strain curves were obtained from bending tests for magnesium AZ31 specimens with and without metal platings. Figure 2 shows stress–strain curves from unplated Mg specimens as well as each of the three types of plating (Zn, Cu, and Ni). While the experiments were performed in the same manner to replicate the results multiple times for most cases, for some cases only one test was performed. Figure 2 only shows a representative curve for different coated samples. As observed in Fig. 2, the stress flow curve differentiates between various plating of Mg specimen.

Table 1 shows the material behavior observed for different plating. Both yield and ultimate tensile strength (UTS) increase for Zn plating, whereas the strength reduces for Cu and Ni plating. The yield and UTS obtained for the unplated sample are 220 MPa and 265 MPa. The Zn plating performed significantly better than the unplated sample, demonstrating a yield strength of 240 MPa and UTS of 295 MPa. The Zn plated sample finally demonstrated a much later onset of softening than the unplated curve, with strength very near its UTS at the end of the test, unlike the

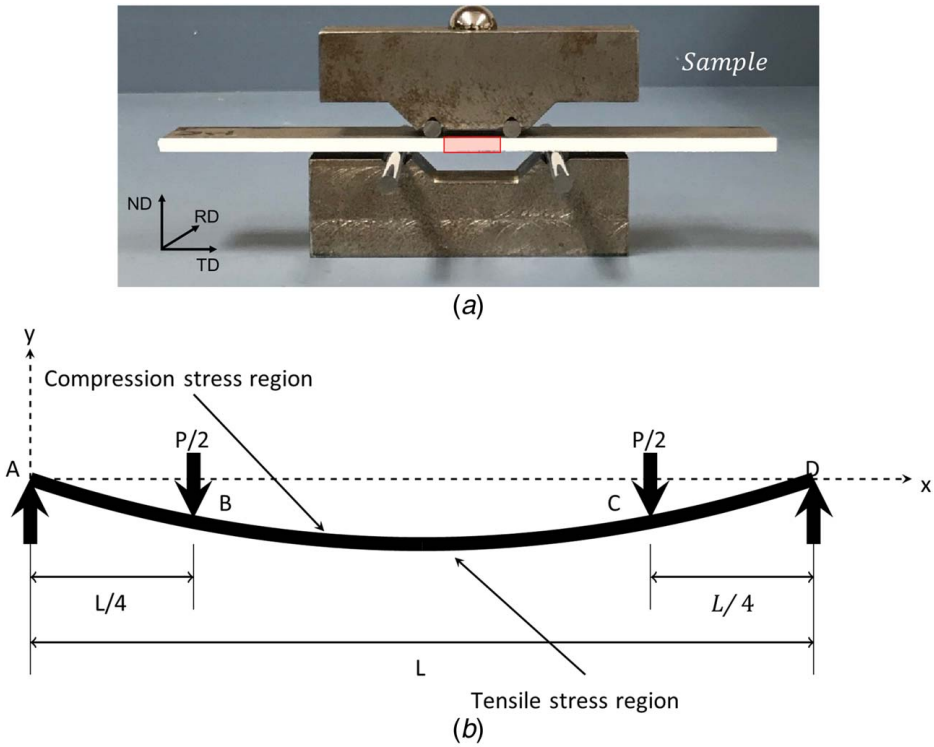

Fig. 1 (*a*) Four-point bending apparatus used for the bend test as well as the rectangular box at the middle of the sample showing field of view for digital image correlation (DIC) analysis and (*b*) a schematic of the symmetric four-point bending test. Notice the tension and compression regions which allows for multiple modes of twinning to occur.

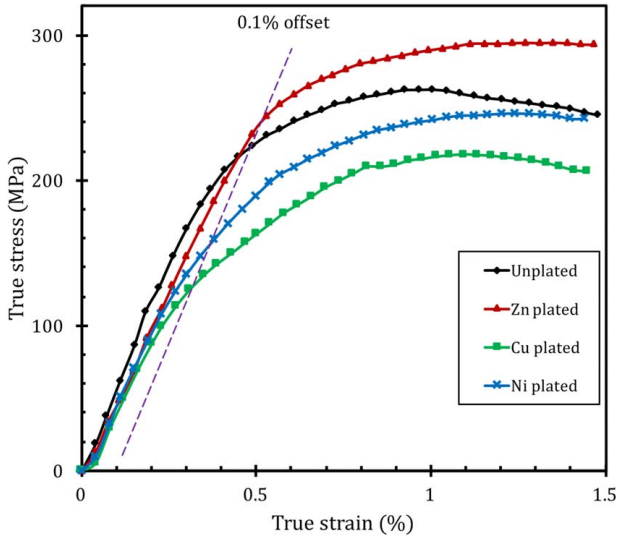

Fig. 2 Plot comparing the stress–strain flow curve for various metal plated magnesium samples with uncoated magnesium specimen. The zinc plated specimen is apparently stronger than any of the other platings.

Table 1 Stress–strain flow properties for magnesium specimens with and without metal platings

Platings	Yield strength (MPa)	Ultimate tensile strength (MPa)	Strain at UTS (ε_{UTS}) (%)
Mg (unplated)	232	265	1.00
Zn plated	244	295	1.31
Cu plated	125	229	1.24
Ni plated	160	248	1.09

unplated sample. On the other hand, the Cu plated and Ni samples actually demonstrated a lower yield strength and UTS than the unplated sample. The Cu plated sample was weaker than the Ni sample with a Cu prestrike.

Samples that were bent to 2% strain were examined under the optical microscope at the same magnification and location on the sample, as seen in Fig. 3. Twin bands are clearly visible in all of the samples. The separation distances between these twin bands and the twin band thickness for each specimen are tabulated in Table 2. The separation and thickness distances were measured along the horizontal directions of observed twin bands, 90 μm from the surface, as indicated by black arrows in Fig. 3. Table 2 clearly shows that twinning was less in the zinc plated sample. The twin bands in the Zn plated sample are thinner, with wider spaces between them. Meanwhile, Ni plated samples showed slightly lower decrease in twin thickness but greater than the Cu plated samples. The chromium conversion proved to have the thickest twin bands on average, followed by the copper and nickel.

Figure 4 shows the strain maps obtained from DIC analysis of four-point bending experiments. The DIC data for Ni samples were corrupted during acquisition, thus DIC analysis of strain field for Ni are not included in Fig. 4. These results showed good agreement with the strain fields from twin bands as observed in the optical microscopy results from Fig. 3 and stress–strain curves in Fig. 2. In particular, the unplated sample showed the most strain in the compression zone, including some banding, while the Zn plated sample showed the least strain. While the strain concentrations were evident at the surface of the Zn plated and the Cu plated samples, the strains in the unplated sample were more homogeneous. The overall plastic strain and the apparent curvature are much greater in the unplated sample than the others even though the samples were all subjected to the same deflection. This indicates that the plating process enhanced detwinning once the applied stress was released.

We calibrated the plastic portion of the stress–strain curve in Fig. 2 with Voce hardening law equation as shown below.

$$\sigma_y = \sigma_0 + R_0\varepsilon^{pl} + R_\infty(1 - \exp(-b\varepsilon^{pl})) \tag{3}$$

where σ_y is the flow stress, ε^{pl} is the plastic strain, and σ_0 corresponds to the stress when plasticity becomes apparent. Meanwhile, R_∞ is the total amount of hardening and b is the hardening decay rate. Figure 5 shows the plastic region of the stress–strain curve fitted with the Voce's hardening law equation. While this does not provide good insight into the underlying physics driving the differences between the results with various coatings, it quantifies the observed differences in yield and hardening parameters. The calibrated values for σ_0, R_0, R_∞, and b are tabulated in Table 3. We set the value of R_0 to zero, assuming that at UTS, all samples behaved similarly. This allowed us to compare the plastic behavior in terms of σ_0, R_∞, and b.

σ_0 appears to be affected by the modulus and crystal lattice of the plating material. While both Mg and Zn have HCP crystal structure, σ_0 increases for the Zn plated sample resulting from the difficulty to nucleate twin at the surface as Zn has a higher modulus than Mg. However, for a similar modulus for Cu and a higher modulus for Ni, σ_0 decreases significantly. On the other hand, the hardening, R_∞, increases considerably for Cu and Ni, but this effect is insufficient to increase their UTS to the levels seen for pure or Zn plated Mg.

Plating with Ni or Cu both led to a lower yield despite their high moduli, contrary to our hypothesis. We theorize that this is due to some effect of the FCC–HCP interface between the plating and the substrate. In particular, we suggest a dislocation transmutation event of the form:

$$2[0\bar{1}1](111)_{FCC} \rightarrow [2\bar{1}\bar{1}\bar{3}]\{2\bar{1}\bar{1}2\}_{HCP} \tag{4}$$

We theorize that due to the highly textured nature of the substrate, the local interface between FCC and HCP will frequently

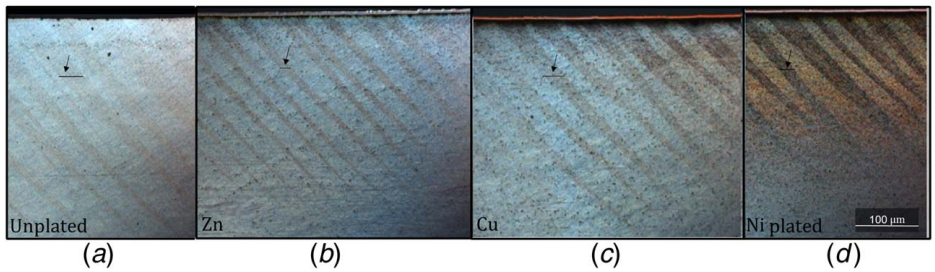

Fig. 3 Optical microscope image of twinning at 2% strain of (*a*) unplated (chromium conversion), (*b*) zinc plated, (c) copper plated, and (*d*) nickel plated Mg. The scale bar for (*a*)–(c) is same as (*d*).

Table 2 Twin band characteristics observed from optical microscopy

Platings	Unplated	Zn plated	Cu plated	Ni plated
Size of twins (μm)	42 ± 7	21 ± 2	35 ± 7	31 ± 10
Twin spacing (μm)	34 ± 10	37 ± 10	35 ± 5	31 ± 5

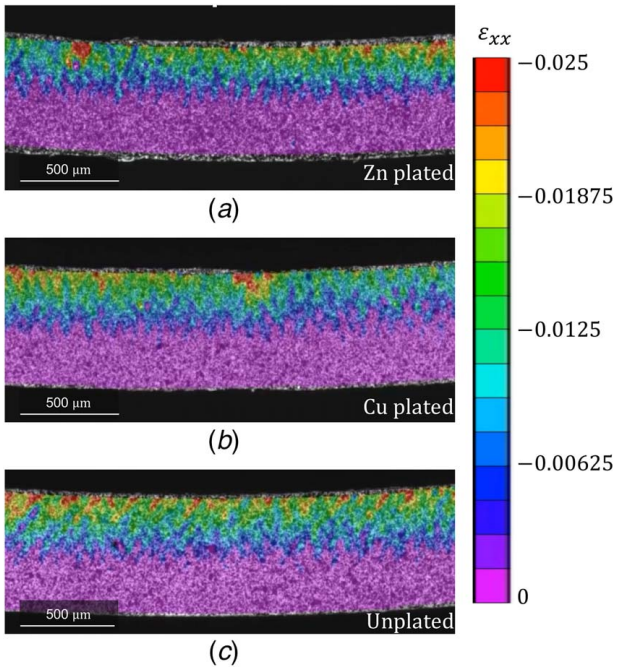

Fig. 4 Digital image correlation (DIC) analysis of (*a*) zinc plated, (*b*) copper plated, and (c) unplated magnesium samples. The strain results show that the electroplating has prevented in localization of twinning induced stress.

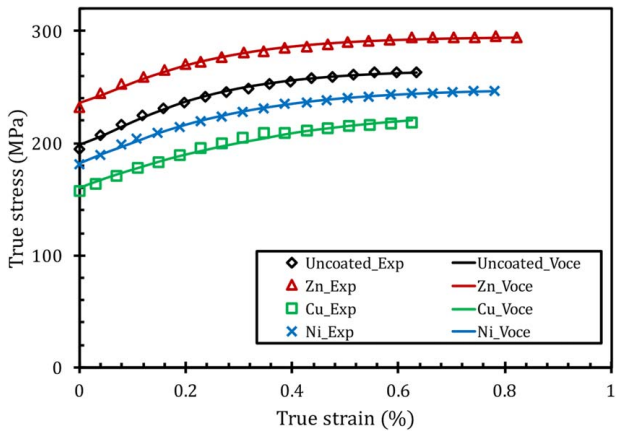

Fig. 5 Stress–strain curves using Voce's hardening law fitted with the plastic portion of experimental data

take the form $\{1\bar{1}1\}_{FCC}||\{0\ \ 0\ \ 0\ \ 1\}_{HCP}$. This aligns other close-packed planes of the FCC plating near the second-order pyramidal plane of the substrate. Dislocations then nucleate from the surface on the {111} planes, move to the interface, and transmute through, combining into $\langle c+a \rangle$ dislocations in the Mg lattice with some defect content left behind at the interface. Since these dislocations nucleating at the surface have a much smaller Burgers vector than $\langle c+a \rangle$ dislocations, they nucleate more easily. $\langle c+a \rangle$ slip has been previously observed to harden extensively, which is compatible with our results showing more hardening with the Cu and Ni plating.

Table 3 Calibrated values of Voce hardening parameters

Plating	Plating lattice	Plating modulus (GPa)	σ_0 (MPa)	R_0 (MPa)	R_∞ (MPa)	b
Mg (unplated)	HCP	44.8	183.0	0	81.5	6.83
Zn plated	HCP	96.4	197.3	0	97.8	6.23
Cu plated	FCC	115	80.0	0	149.4	3.98
Ni plated	FCC	200	106.7	0	141.4	5.32

Alternatively, it is possible that enhanced twin nucleation at the phase boundary is responsible for the lower yield in Cu and Ni, followed by detwinning upon the release of stress. This process could be partially accommodated by slip in the plating. Further investigation will be needed to identify whether these processes occur.

Plating with Zn, which does not produce a FCC–HCP interface, appeared to have the anticipated effect. The HCP–HCP interface between Zn and Mg restricts plasticity rather than providing a nucleation site like the FCC–HCP interface. Twinning was suppressed, increasing both the yield and ultimate stresses. Overall, the effect of plating in all cases led to decreased twinning, increased detwinning, and increased hardening.

4 Conclusion

In summary, zinc plating seemed to discourage twin nucleation and thus delay yield and increase the strength of Mg AZ31. Not only was twin nucleation more infrequent, but twin thickening was also inhibited compared to an unplated sample with the same loading. It is theorized that this occurs because the Zn plating presents a hard surface barrier preventing the kinking of the surface necessary for the twin to nucleate. If this result is confirmed, it could lead to significant improvements in Mg alloy strength. Unlike slip, twinning produces highly localized deformation, which is specifically retarded by the stiff plate of Zn. Experiments with plating by Cu instead of Zn showed an opposite effect with earlier yield, even though twins still appear to be suppressed. The results show that Zn is specifically effective as a coating to strengthen Mg surfaces because Zn has excellent adherence to the Mg substrate and significantly higher stiffness than Mg.

Acknowledgment

The research described and the resulting data presented herein, unless otherwise noted, were funded under PE 0602784A, Project T53 "Military Engineering Applied Research," Topic 3 under Contract W56HZV-17-C-0095, managed by the US Army Engineer Research and Development Center. The work described in this document was conducted in the Center for Advanced Vehicular Systems at Mississippi State University. OPSEC permission was granted to publish this information.

Conflict of Interest

There are no conflicts of interest. This article does not include research in which human participants were involved. Informed consent was obtained for all individuals. Documentation provided upon request. This article does not include any research in which animal participants were involved.

Data Availability Statement

The datasets generated and supporting the findings of this article are obtainable from the corresponding author upon reasonable request.

References

[1] Barnett, M. R., Nave, M. D., and Bettles, C. J., 2004, "Deformation Microstructures and Textures of Some Cold Rolled Mg Alloys," Mater. Sci. Eng. A, **386**(1–2), pp. 205–211.

[2] Agnew, S. R., Yoo, M. H., and Tomé, C. N., 2001, "Application of Texture Simulation to Understanding Mechanical Behavior of Mg and Solid Solution Alloys Containing Li or Y," Acta Mater., **49**(20), pp. 4277–4289.

[3] Sandlöbes, S., Zaefferer, S., Schestakow, I., Yi, S., and Gonzalez-Martinez, R., 2011, "On the Role of Non-Basal Deformation Mechanisms for the Ductility of Mg and Mg–Y Alloys," Acta Mater., **59**(2), pp. 429–439.

[4] Baird, J. C., Li, B., Parast, S. Y., Horstemeyer, S. J., Hector, L. G., Jr., Wang, P. T., and Horstemeyer, M. F., 2012, "Localized Twin Bands in Sheet Bending of a Magnesium Alloy," Scr. Mater., **67**(5), pp. 471–474.

[5] El Kadiri, H., and Oppedal, A., 2010, "A Crystal Plasticity Theory for Latent Hardening by Glide Twinning Through Dislocation Transmutation and Twin Accommodation Effects," J. Mech. Phys. Solids, **58**(4), pp. 613–624.

[6] Oppedal, A., El Kadiri, H., Tomé, C., Kaschner, G., Vogel, S. C., Baird, J., and Horstemeyer, M., 2012, "Effect of Dislocation Transmutation on Modeling Hardening Mechanisms by Twinning in Magnesium," Int. J. Plast., **30**, pp. 41–61.

[7] Sun, D., Ponga, M., Bhattacharya, K., and Ortiz, M., 2018, "Proliferation of Twinning in Hexagonal Close-Packed Metals: Application to Magnesium," J. Mech. Phys. Solids, **112**, pp. 368–384.

[8] Anderson, P. M., Hirth, J. P., and Lothe, J., 2017, *Theory of Dislocations*, Cambridge University Press, New York.

[9] Nave, M. D., and Barnett, M. R., 2004, "Microstructures and Textures of Pure Magnesium Deformed in Plane-Strain Compression," Scr. Mater., **51**(9), pp. 881–885.

[10] Jiang, L., Jonas, J. J., Luo, A. A., Sachdev, A. K., and Godet, S., 2006, "Twinning-Induced Softening in Polycrystalline Am30 Mg Alloy at Moderate Temperatures," Scr. Mater., **54**(5), pp. 771–775.

[11] Yoo, M., 1981, "Slip, Twinning, and Fracture in Hexagonal Close-Packed Metals," Metall. Trans. A, **12**(3), pp. 409–418.

[12] Christian, J. W., and Mahajan, S., 1995, "Deformation Twinning," Prog. Mater. Sci., **39**(1–2), pp. 1–157.

[13] Hartt, W., and Reed-Hill, R., 1968, "Internal Deformation and Fracture of Second-Order $\{10\bar{1}1\}-\{10\bar{1}2\}$ Twins in Magnesium," NASA Technical Reports Server (NTRS), Document ID 19680051952.

[14] Kannan, V., Hazeli, K., and Ramesh, K. T., 2018, "The Mechanics of Dynamic Twinning in Single Crystal Magnesium," J. Mech. Phys. Solids, **120**, pp. 154–178.

[15] El Kadiri, H., Kapil, J., Oppedal, A., Hector, L., Jr., Agnew, S. R., Cherkaoui, M., and Vogel, S., 2013, "The Effect of Twin–Twin Interactions on the Nucleation and Propagation of $\{10\bar{1}2\}$ Twinning in Magnesium," Acta Mater., **61**(10), pp. 3549–3563.

[16] Paudel, Y., Giri, D., Priddy, M. W., Barrett, C. D., Inal, K., Tschopp, M. A., Rhee, H., and El Kadiri, H., 2021, "A Review on Capturing Twin Nucleation in Crystal Plasticity for Hexagonal Metals," Metals, **11**(9), p. 1373.

[17] Russell, W. D., Bratton, N. R., Paudel, Y., Moser, R. D., McClelland, Z. B., Barrett, C. D., Oppedal, A. L., et al., 2020, "In Situ Characterization of the Effect of Twin-Microstructure Interactions on {1 0 1 2} Tension and {1 0 1 1} Contraction Twin Nucleation, Growth and Damage in Magnesium," Metals, **10**(11), p. 1403.

[18] Paudel, Y., Barrett, C. D., Tschopp, M. A., Inal, K., and El Kadiri, H., 2017, "Beyond Initial Twin Nucleation in hcp Metals: Micromechanical Formulation for Determining Twin Spacing During Deformation," Acta Mater., **133**, pp. 134–146.

[19] Paudel, Y., Indeck, J., Hazeli, K., Priddy, M. W., Inal, K., Rhee, H., Barrett, C. D., Whittington, W. R., Limmer, K. R., and El Kadiri, H., 2020, "Characterization and Modeling of $\{10\bar{1}2\}$ Twin Banding in Magnesium," Acta Mater., **183**, pp. 438–451.

[20] Wang, J., Beyerlein, I. J., and Tomé, C. N., 2010, "An Atomic and Probabilistic Perspective on Twin Nucleation in Mg," Scr. Mater., **63**(7), pp. 741–746.

[21] Zhu, S., and Ringer, S. P., 2018, "On the Role of Twinning and Stacking Faults on the Crystal Plasticity and Grain Refinement in Magnesium Alloys," Acta Mater., **144**, pp. 365–375.

[22] Barrett, C. D., Imandoust, A., Oppedal, A. L., Inal, K., Tschopp, M. A., and El Kadiri, H., 2017, "Effect of Grain Boundaries on Texture Formation During Dynamic Recrystallization of Magnesium Alloys," Acta Mater., **128**, pp. 270–283.

[23] Hazeli, K., Sadeghi, A., Pekguleryuz, M., and Kontsos, A., 2013, "The Effect of Strontium in Plasticity of Magnesium Alloys," Mater. Sci. Eng. A, **578**, pp. 383–393.

[24] Bhuiyan, M. S., and Mutoh, Y., 2011, "Corrosion Fatigue Behavior of Conversion Coated and Painted az61 Magnesium Alloy," Int. J. Fatigue, **33**(12), pp. 1548–1556.

[25] Arcieri, E. V., Baragetti, S., and Borzini, E., 2018, "Bending Fatigue Behavior of 7075-Aluminum Alloy," *Key Engineering Materials*, Vol. 774, Trans Tech Publ, pp. 1–6.

[26] Hsiao, H.-Y., and Tsai, W.-T., 2005, "Characterization of Anodic Films Formed on az91d Magnesium Alloy," Surf. Coat. Technol., **190**(2–3), pp. 299–308.

[27] Lee, Y., Chu, Y., Chen, F., and Lin, C., 2013, "Mechanism of the Formation of Stannate and Cerium Conversion Coatings on az91d Magnesium Alloys," Appl. Surf. Sci., **276**, pp. 578–585.

[28] Wang, Z., Jia, F., Yu, L., Qi, Z., Tang, Y., and Song, G.-L., 2012, "Direct Electroless Nickel–Boron Plating on az91d Magnesium Alloy," Surf. Coat. Technol., **206**(17), pp. 3676–3685.

[29] Huang, C., Wang, T., Weirich, T., and Neubert, V., 2008, "A Pretreatment With Galvanostatic Etching for Copper Electrodeposition on Pure Magnesium and Magnesium Alloys in an Alkaline Copper-Sulfate Bath," Electrochim. Acta, **53**(24), pp. 7235–7241.

[30] Huang, C. A., Lin, C. K., and Yeh, Y. H., 2010, "Increasing the Wear and Corrosion Resistance of Magnesium Alloy (az91d) With Electrodeposition From Eco-Friendly Copper- and Trivalent Chromium-Plating Baths," Surf. Coat. Technol., **205**(1), pp. 139–145.

[31] Huang, C. A., Chuang, C. H., Yeh, Y. H., You, C. Y., and Hsu, F.-Y., 2016, "Low-Cycle Fatigue Fracture Behavior of a Mg Alloy (az61) After Alkaline Cu, Alkaline Followed by Acidic Cu, Ni/Cu, and Cr-C/Cu Electroplating," Mater. Sci. Eng. A, **662**, pp. 111–119.

[32] Chen, Y., Shao, S., Liu, X.-Y., Yadav, S. K., Li, N., Mara, N., and Wang, J., 2017, "Misfit Dislocation Patterns of Mg-Nb Interfaces," Acta Mater., **126**, pp. 552–563.

[33] Zhang, Y., Millett, P. C., Tonks, M., and Biner, B., 2012, "Deformation-Twin-Induced Grain Boundary Failure," Scr. Mater., **66**(2), pp. 117–120.

[34] Young, W., 1989, "Elastic Stability Formulas for Stress and Strain," Roark's Formulas for Stress and Strain, 6th ed., McGraw-Hill, New York, NY, p. 688.